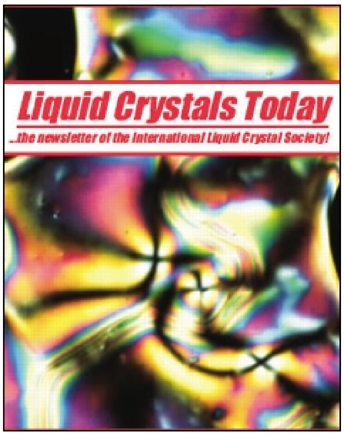

Liquid Crystals Today
Publication details, including instructions for authors and subscription information:
http://www.informaworld.com/smpp/title~content=t713681230

Important Physical Properties of Smectic Liquid Crystals[1]

M. J. Towler[a]; H. G. Walton[a]; I. W. Stewart[b]
[a] Sharp Laboratories of Europe Ltd., Oxford Science Park, Oxford, England [b] Department of Mathematics, University of Strathclyde, Glasgow, Scotland

To cite this Article Towler, M. J. , Walton, H. G. and Stewart, I. W.(1998) 'Important Physical Properties of Smectic Liquid Crystals[1]', Liquid Crystals Today, 8: 1, 5 — 9
To link to this Article: DOI: 10.1080/13583149808047692
URL: http://dx.doi.org/10.1080/13583149808047692

17 Takeda, B., 1930, *Techn. Rep. Tohoku Univ.*, **9,** 447.

18 Oberhoffer, P., 1924, *Stahl u. Eisen*, **44,** 979.

19 Wever, F., 1925, *Stahl u. Eisen*, **45,** 1208.

20 Maurer, E., 1925, *Stahl u. Eisen*, **45,** 1629.

21 Haughton, J. L., 1927, *J. Iron Steel Inst.*, **115,** 417.

22 Bain, E. C., 1926, *Trans. Amer. Soc. Steel Treating*, **9,** 9.

23 Sykes, W. P., 1926, *Trans. Amer. Soc. Steel Treating*, **10,** 839.

24 Wever, F., 1926, *Z. Anorg. Chem.*, **154,** 294.

25 Isawa, M., and Murakami, T., 1927, *Kinzoku-no-Kenkyu*, **4,** 467.

26 Roe, W. P., and Fishel, W. P., 1952, *Trans. ASM*, **44,** 1030.

27 Wever, F., 1928/29, *Arch. Eisenhüttenwes.*, **2,** 739.

28 Wever, F., and Müller, A., 1929, *Mitt. Kais. Wilh.-Inst. Eisenforschg.*, **11,** 193.

29 Cladis, P., 1988, *Mol. Cryst. Liq. Cryst.*, **165,** 85.

30 Valasek, J., 1921, *Phys. Rev.*, **17,** 475.

31 Fertig, W. A., Johnston, D. C., DeLong, L. E., McCallum, R. W., Maple, M. B., and Matthias, B. T., 1977, *Phys. Rev. Lett.*, **38,** 987.

32 Cladis, P., 1998, *Handbook of Liquid Crystals*, edited by D. Demus, J. Goodby, G. W. Gray, H.-W. Spiess, and V. Vill (Weinheim: Wiley-VCH), to appear.

Important Physical Properties of Smectic Liquid Crystals[1]

M. J. Towler,[†]
H. G. Walton[†] and
I. W. Stewart[††]

[†]Sharp Laboratories of Europe Ltd., Oxford Science Park, Oxford OX4 4GA, England

[††]Department of Mathematics, University of Strathclyde, Glasgow G1 1XH, Scotland

Introduction

The surface stabilized ferroelectric liquid crystal (SSFLC) device [1] is seen as a promising candidate for future flat panel displays. Its sub-millisecond response time and bistable switching characteristics are attractive features not present in the commonly encountered TN (Twisted Nematic) and STN (Super-Twisted Nematic) displays. A mature ferroelectric display technology has been slow to develop however. One reason for this is the greater difficulties in determining the important parameters which dictate the behaviour of smectic phases. Whilst the viscoelastic equations describing the behaviour of nematics [2] have been extensively studied, the more complicated smectic equations have been explored in only a limited number of instances. The more highly broken symmetry of the smectic C* phase, deriving from the existence of molecular layering, results in many new physical phenomena not observable in nematics. For example, complicated layer defects can occur in smectics (by definition an impossibility in nematics); new fluid flow phenomena can occur, related to the anisotropy in flowing across, as opposed to within layers; and the broken symmetry of the Sm-C* phase requires the introduction of a biaxial dielectric permittivity tensor (rather than the uniaxial nematic tensor). In this article we expand on these examples, highlighting some essential physics for the non-specialist and pointing out some areas of relevance to display technology.

Alignment in finite thickness samples: chevron states

In an infinite sample, the Sm-A liquid crystal phase is characterized by molecules adopting a layered structure with molecules aligned on average along the layer normal. The Sm-C phase is characterized by molecules everywhere tilted at some equilibrium angle, θ, with respect to the layer normal, allowing them to lie anywhere on the surface of a cone of apex 2θ. Confining a smectic to a finite volume can considerably complicate the layering geometry. In practical devices it is important to understand the layer structure both to optimize device switching times and to minimize the presence of layer defects.

We begin by considering a Sm-A confined between parallel, zero pretilt, rubbed surfaces (figure 1). A transition to the Sm-C requires that the layers adopt a chevron structure in order that molecules can satisfy the mutual constraints of (i) lying at the tilt angle, θ, with respect to the layer normal and (ii) maintaining the layer periodicity of the overlying Sm-A phase at the surfaces, which arises as a consequence of molecular adsorption ('surface pinning') in the Sm-A phase [3].

There are two directions in which the chevron apex may point, characterized by opposite sign of the layer tilt angle δ. States of positive δ are denoted 'C1' and states of negative δ 'C2' [4]. For a zero pretilt cell these states are clearly equivalent and we can expect both to occur with equal probability. Practically, the existence of both chevron states in a display is undesirable, as a region of C1 meets a region of C2 at a 'zig-zag' defect which scatters light and reduces optical contrast.

The symmetry between the energy of C1 and C2 states can be broken if we introduce surface pretilt, although this results in a further degree of complexity in layer structure. It is illustrative to consider a specific example: consider a cell of finite pretilt, ψ, in which we constrain molecules to lie at some cone angle θ throughout the cell thickness. Furthermore, for concreteness, we suppose that molecules at the surface are constrained

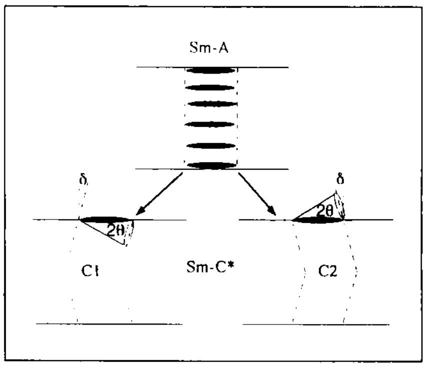

Figure 1. The Sm-A to C transition with zero pretilt showing equivalence of the C1 and C2 states.

to lie along the rubbing direction (drawn in the plane of the page, i.e. ϕ=90° in figure 2). Figure 2 (left) shows how layers must be tilted in the C2 state to satisfy these mutual constraints. If we now consider the C1 (i.e. positive δ) state, we find that in order for molecules to both lie at the pretilt angle and match the Sm-A layer pitch at the surface, we must either:

(i) allow molecules near the surfaces to pull away from the rubbing direction and rotate around the cone to ϕ=90° (i.e. assume 'constant-θ/variable-φ')

(ii) relax the constraint that the cone angle is constant near the surface ('variable-θ/fixed-ϕ(=90°)'^{2}, which is equivalent to allowing layers to bend as they approach the surface).

There is the further possibility that we adopt neither model and instead introduce defects into the sample^3. In the absence of a detailed understanding of the nature of such defects however, we shall not consider this option further.

The 'constant-θ/variable-φ' has been widely considered [4] and does produce some qualitatively correct predictions. It is a straightforward exercise in geometry to show that for this model we must have

$$\sin(\varphi)=\tan(\delta+\psi)/\tan(\theta) \text{ for C2 and}$$
$$\sin(\varphi)= -\tan(\delta-\psi)/\tan(\theta) \text{ for C1}$$

Clearly in the first equation, if the pretilt $\psi>\theta-\delta$ the C2 state cannot exist (there is no solution $\sin(\phi)>1$). Experimentally it is confirmed that high pretilt surfaces favour the formation of C1 and low pretilts favour C2, in agreement with a fixed-θ model.

What is less clear however, is that it is indeed energetically favourable for molecules to follow this model and pull away from the alignment direction, rather than varying θ near a rubbed surface. In addition, it is sometimes experimentally observed that although a given material on a surface may show 100% C2 at some temperature, a second structurally similar material, which one would expect to show similar surface interactions, will align as a mixture of C1 and C2. We show here that adopting a 'variable-θ/fixed-ϕ(= 90°)' model predicts the importance of two material parameters in governing the relative stability of C1 and C2.

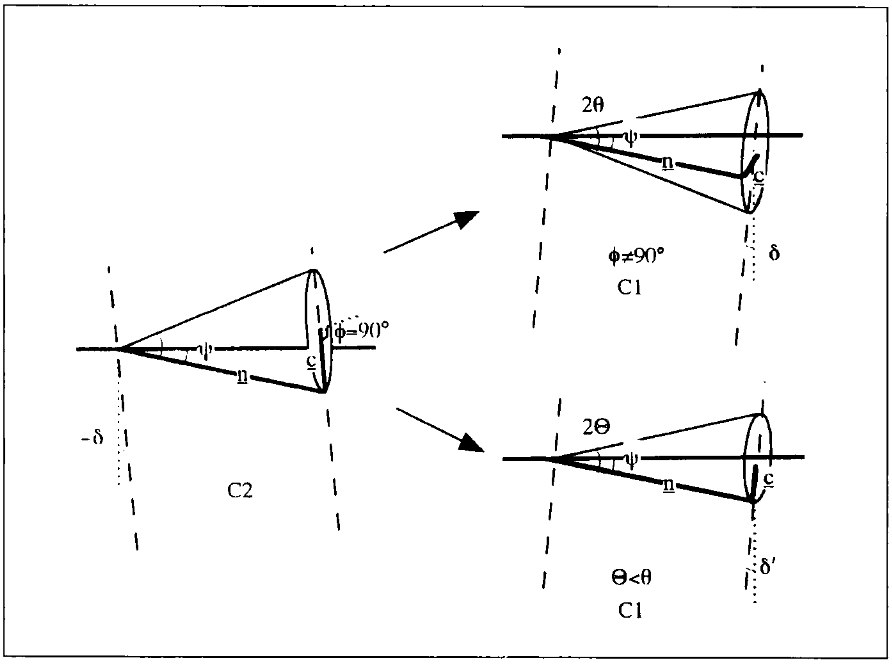

Figure 2. (Left) C2 with a fixed surface layer pitch, |δ|, ψ and φ=90°. (Right) C1 (i.e. positive δ) state for the same surface layer pitch and ψ. Position on the cone can be described by ϕ or we can introduce a vector **c**. Upper C1 diagram illustrates 'variable φ' model, whilst in lower ('variable θ') diagram δ' is not constant near the surface.

Assuming constant ϕ and letting z be the distance through the sample we can write a simple phenomenological expression for the free energy density W_d of a Sm-C as:

$$W_d \approx \frac{A}{2}\left(\frac{d\theta(z)}{dz}\right)^2 + \frac{K}{4}\left(\theta(z)^2-\theta_e^2\right)^2 \quad (1)$$

The first term in this equation describes the bending of smectic layers which must accompany distortions of the cone angle in order that the layer pitch remains constant through the cell. 'A' is an elastic constant relating to the stiffness of the layers. The second term describes the inherent desire of the system to sit at some bulk equilibrium cone angle θ_e. Distorting to some new value, θ, near a surface requires energy which can be approximated by a series (Landau) expansion, 'K' being a constant Landau parameter. To determine the equilibrium variation of θ we minimize this free energy, resulting in a (Euler Lagrange) differential equation for $\theta(z)$, which can then be solved subject to the appropriate boundary conditions for θ in the C1 and C2 states (obtained by straightforward geometrical considerations). Having found the $\theta(z)$ (actually $\approx\tanh(z/l)$ ignoring constants, where l is the penetration length defined below) which minimizes the energy of the C1 and C2 states, we can simply integrate equation (1) to find the total energy of these states. The result is:

$$(C1-C2)energy \sim \theta_e^3 K\left(\frac{A}{K}\right)^{1/2}$$

(We could perhaps have arrived at this equation directly by noting that equation (1) is formally equivalent to the well known 'kink equation' widely used in condensed matter physics to model domain walls [5].)

Thus the variable cone angle model suggests the importance of two material parameters:

(i) The Landau parameter, K
(ii) The penetration length scale $l=(A/K)^{1/2}$.

We are not aware of any experiments which have been performed to test these predictions.

FLC switching and dielectric biaxiality

A schematic illustration of the switching time (τ)-voltage (V) characteristic of a typical low spontaneous polarization (P_s) SSFLC is shown in figure 3 [6].

SSFLC devices are multiplex addressed one line at a time [7]. This leads to a requirement that the curve in figure 3 has steep sides. Furthermore, for optimizing display contrast, certain drive schemes require that we operate at voltages above V_{min} [8]. Clearly then, it is desirable that we understand the material parameters that dictate the shape of the τ-V curve.

The existence of a minimum in the switching curve arises from competition between the different torques acting on an FLC molecule in an electric field, **E**. At low fields switching is dominated by the (linear) interaction between **E** and the P_s:

$$\text{polarization torque} \sim P_s|\mathbf{E}| \sin\phi.$$

At high fields, switching is dominated by the (quadratic) dielectric torque:

$$\text{dielectric torque} \sim \varepsilon_0 (\varepsilon\, \mathbf{E})\times\mathbf{E}$$

Here ε is the (tensor) dielectric anisotropy of the molecules. Dielectric torques are of course responsible for nematic switching, unlike for nematics however, for which ε has only two components, one parallel and the other perpendicular to the director, the C_2 symmetry of FLCs demands that we consider a biaxial ε with three independent components: ε_1 along the director, ε_2 normal to the director and tangential to the cone and ε_3 orthogonal to these two.

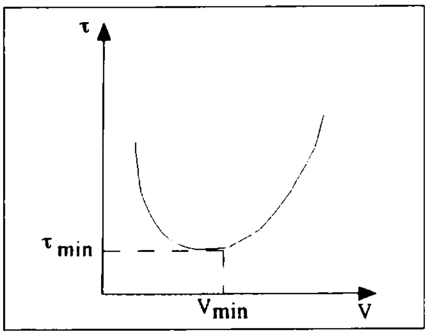

Figure 3. Schematic τ–V curve for lower P_S material.

If we ignore flow and elastic terms we can calculate the dynamic motion of a FLC molecule around the cone in an eletric field by setting the difference of the above torques equal to the time rate of change of the angle φ multiplied by a suitable rotational viscosity constant (in the literature denoted: $\lambda_5 \sim \gamma \sin^2\phi$ [9]). We can then solve this equation to find ϕ as a function of time. It can be shown [10] that:

$$E_{min} \sim P_s/\,\delta\varepsilon \text{ and } \tau_{min} \sim \lambda_5 .\ \delta\varepsilon/P_s^2$$

(where $\delta\varepsilon=\varepsilon_2-\varepsilon_1$). Practically, P_s is readily tuned by modifying the amount of chiral dopant in a non-chiral Sm-C host. Increasing $\delta\varepsilon$ requires the addition of lateral dipoles to molecules, although in doing so we must try to avoid overly increasing their rotational viscosity. Recently Sakigawa *et al.* [11] have elegantly confirmed the simple model above by systematically varying $\delta\varepsilon$ in a two component host, chirally doping and measuring the resultant E_{min} (see results in figure 4).

Permeative flow in smectic liquid crystals

So far in our discussion we have ignored flow. Smectics however exhibit fascinating and unusual hydrodynamic phenomena deriving from the existence of the periodic layering. Flow within layers is liquid-like (described by the 'Navier–Stokes' equation), whilst attempts to flow across layers ('permeation') are governed by a separate law (Darcy's law) [12, 13]. Here we consider what happens when material in a Sm-A phase attempts to flow past a barrier [14].

Without performing explicit calculations we can guess at the behaviour we may observe in the situation depicted in figure 5. In region A layers are subjected to a dilative force since material is having to flow out across the layers. It is well known that when we try to pull smectic layers apart they buckle in an attempt to fill space [15, 16]. Thus in region A we expect to observe buckling of layers, which will be visible through the scattering of light. In region B layers are subject to compression due to the inflow of material. Sm-A layers can only compress by tilting the molecules within them and since this is normally energetically costly, therefore we may commonly witness no effects in region B. If however, the temperature approaches an underlying Sm-C phase, the energetic cost of inducing tilt becomes vanishingly small (the Sm-A to Sm-C transition is second order) and we can expect to witness a flow-induced phase transition to the Sm-C in region B. Finally, since the total number of layers along z must be conserved (assuming edge dislocation defects are not created by our flow), just outside the dilated region A we can expect regions of compression and vice versa for region B. The actual shape of the compressed and dilated regions is to be determined through calculation.

Experiment [16] beautifully confirms these expectations (figure 6).

We can go further and derive an analytic expression for the flow profile.

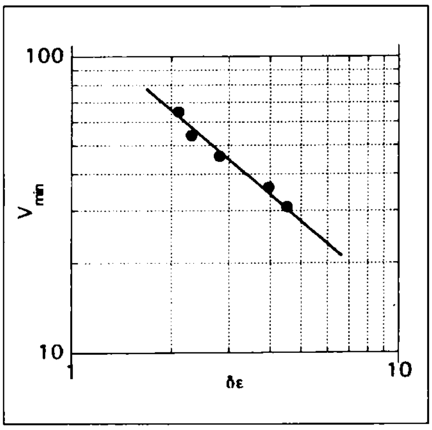

Figure 4. Experimental results [11] showing the effect of dielectric biaxiality on V_{min}.

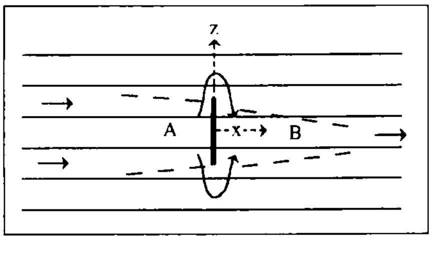

Figure 5. Schematic diagram of flow (from left to right) past a barrier in the Sm-A. 'A' and 'B' are regions of layer dilation and compression respectively.

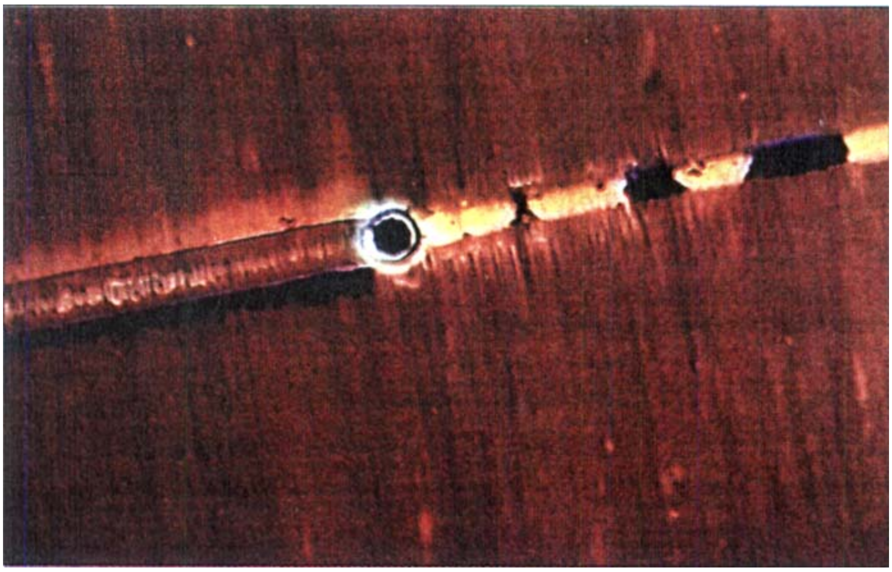

Figure 6. Photomicrograph between crossed polarizers of flow (from left to right) past a 50 µm diameter pillar in Sm-A ($T-T_{AC}$=0.4°C), showing white (i.e. scattering) regions of layer buckling due to layer dilation, and coloured regions of compression-induced tilt (note the appearance of Sm-C domains of opposite tilt sign in the compressed region to the right of the barrier). Differing flow birefringence colours are observed in the compressed regions to the left of the barrier, due to the opposite sign of flow gradient in these regions.

Assuming flow is confined to the x–z plane, and that there are no sources or sinks of material we can write:

$$\frac{\partial P}{\partial z}=\frac{-V_z}{\lambda_p},\qquad \frac{\partial P}{\partial x}=\eta_3\frac{\partial^2 V_x}{\partial z^2},$$

$$\frac{\partial V_x}{\partial x}+\frac{\partial V_z}{\partial z}=0$$

The first of these equations describes the velocity with which material flows in the *z* direction as depending upon the pressure gradient acting in that direction (Darcy's law). This meets with our experience, since in that direction the smectic appears crystalline. The second equation, containing mixed spatial derivatives, describes liquid-like flow in the *x* direction: the drag which a small portion of a fluid experiences when trying to flow depends upon its velocity relative to the fluid either side of it. The third equation expresses our basic assumption of incompressibility i.e. that at any instant any material entering a region must be balanced by an equal amount of material leaving the region.

The task of determining the shape of the flow profile in figure 5 is now reduced to solving these three coupled equations to find v_x and v_z, given the boundary conditions that both must be zero on the surface of the barrier and that v_z->0 a long distance directly above or below barrier in the *z* direction. Figure 7 shows the parabolic nature of the flow profile behind a barrier, calculated from analytic solutions for v_x and v_z [17]. Clearly the derived flow profile shows a striking similarity with the results of the experiment in figure 7.

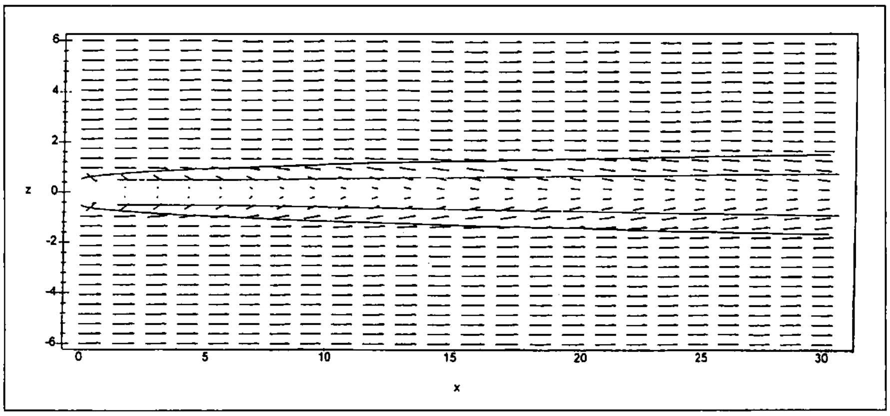

Figure 7. Calculated flow profile behind a barrier. The barrier at *z*=*x*=0 is normalized to height *z*=±0.5, and the short half-arrow lines represent the velocity vector. The continuous outer lines represent a parabolic boundary layer for which the *z*-component of the velocity is small.

Conclusion

Despite over two decades of research, the physics of smectic liquid crystals still contains many fascinating and poorly understood areas of fundamental scientific interest. In addition, with a growing demand for large area, high resolution flat panel displays, smectic devices such as the SSFLC, AFLC (Antiferroelectric Liquid Crystal) [18] and TAFLC (Thresholdless Antiferroelectric Liquid Crystal) [19] are increasingly important to the LCD industry. A detailed understanding of the underlying physics of these phases will be necessary if successful products based on smectics are to be realized.

Notes

1 First presented at London Mathematical Society Symposium on Mathematical Models of Liquid Crystals and Related Polymeric Systems, Durham, July 1995.

2 Strictly we should consider the possibility that both ϕ and θ vary near the surface. For the purposes of gaining physical insight and avoiding mathematcial compexity however, it is sufficient to discuss the two limiting possibilites.

3 The notion of layer defects could be generalized to consider the possibility that layer melting (i.e. a reduction in order parameter occurs as we approach the surface), by introducing a suitable free energy expression containing terms in gradients of the order parameter.

References

1 Clark, N. A., and Lagerwall, S. T., 1980, *Appl.Phys.Lett.*, **36**(1), 89.
2 Leslie, F. M., 1966, *Quart. J. Mech. appl. Math.*, **19**, 357.
3 Cagnon, M., and Durand, G., 1993, *Phys. Rev. Lett.*, **70**(18), 2742.
4 Kanabe, J., Inoue, H., Mitzutome, A, Hanyru, Y., Katagari, K., Yoshihara, S., 1991, *Ferroelectrics*, **114**, 3.
5 Chaikin, P. M., and Lubensky, T. C., *Principles of Condensed Matter Physics* (Cambridge: Cambridge University Press), p. 597.

6 Saunders, F. C., Hughes, J. R., Pedlingham, H. A., and Towler, M. J., 1989, *Liq. Cryst.*, **6**, 341.

7 e.g. Dijon, J., 1990, Liquid Crystals : *Applications and Uses*, edited by Birenda Bahadur (Singapore: World Scientific).

8 Surguy, P. W., Ayliffe, P. J., Birch, M. J., Bone, M. F., Coulsen, I., Crossland, W. A., Hughes, J. R., Ross, P. W., Saunders, F. C., and Towler, M. J., 1991, *Ferroelectrics*, **122**, 63.

9 Leslie, F. M., Stewart, I. W., Nakagawa, M., 1991, *Mol. Cryst. Liq. Cryst.*, **198**, 443.

10 Towler, M. J., Jones, J. C., and Raynes, E. P., 1991, *Liq.Cryst.*, **11**, 365.

11 Sakigawa, A., Ito, N., Koden, M., 1995, *Proceedings of 21st Liquid Crystal Conference in Japan*, Sendai.

12 Martin, P. C., Parodi, O., and Pershan, P. S., 1972, *Phys. Rev.* A, **6**, 2401.

13 de Gennes, P. G., 1974, *Phys. Fluids*, **17**, 9.

14 Clark, N. A., 1978, *Phys.Rev.Lett.* **40**, 1663.

15 Ribotta, R., and Durand, G., 1977, *J. Phys.* (France), **38**, 179.

16 de Gennes, P. G., and Prost, J., 1993, *The Physics of Liquid Crystals* (Pergamon).

17 Walton, H. G., Stewart, I. W., and Towler, M. J., 1996, *Liq. Cryst.*, **20**(5), 665.

18 Yamada, Y., Yamamoto, N., Nakamura, S., Koshobu, N., Ohmi, S., Sato, R., Aoki, K., and Imai, S., 1995, *SID Int. Symp. Digest Tech. Papers*, **26**, 789.

19 Yoshida, T., Tanaka, T., Ogura, J., Wakai, H., and Aoki, H., 1997, *SID Int. Symp. Digest Tech. Papers*, **28**, 841.

PRODUCT NEWS

Sharp Announces Big Improvements in Performance for STN Displays

Sharp has launched a new display series featuring its Triple Super Twisted Nematic (TSTN) cell structure together with a dual scan drive method to give high contrast and very fast response. The LM6Q33 illustrated features 80 ms response time, 40:1 contrast ratio and 180 cd m^{-2} brightness. This enables bright video pictures to be displayed with almost no noticeable ghosting at video frame rates in excess of 30 fps.

For further information contact:

Daniel Reinhardt
Media Concept Öffentlichkeitsarbeit Fischer-Appelt GmbH
Bornkampsweg 2
D-22761 Hamburg, Germany
email: dr@media-concept.de
Fax: + 49 40 899 699-30

Brilliant video performance with the new 5.5 inch $^1/_4$ VGA CSTN panel: using DualScan technology the LM6Q33 features a response time of no more than 80 ms.

COMPANY NEWS

UK Display Technology Alliance

One of the initiatives stimulated by the UK Government-sponsored Technology Foresight exercise is the formation of the UK Display Technology Alliance (DTA). This is a consortium of around 20 organizations involved with research and development of flat panel displays and related technologies. The consortium is led by CRL, and comprises 9 major companies, 5 small or medium-sized enterprises and 6 UK universities. Under the initial 3 year programme a number of technical objectives will be pursued which will be of benefit to the displays industry. The projects embrace a number of display technologies, but work to enhance LCDs includes the use of novel optical substrates and films, the development of thin and/or flexible substrates for flat panel displays, improved manufacturing techniques for the connection of drive electronics and the development of field emission backlights. In addition to these technical projects, the DTA plans to hold a series of technical workshops and publishes a regular newsletter called Display Focus.

For further information contact:

Dr A Mosley,
CRL, Dawley Road,
Hayes, Middlesex, UB3 1HH
email: dta@crl.co.uk
fax: + 44-181-848-6653